

# Spontaneous quantum Hall effect in quarter-doped Hubbard model on honeycomb lattice and its possible realization in quarter-doped graphene system

Tao Li

*Department of Physics, Renmin University of China, Beijing 100872, P.R.China*

(Dated: July 5, 2018)

We show that as the result of the nesting property of the Fermi surface, the quarter-doped Hubbard model on honeycomb lattice is unstable with respect to the formation of a magnetic insulating state with nonzero spin chirality for infinitesimally small strength of electron correlation. The insulating state is found to be topological nontrivial and to have a quantized Hall conductance of  $\sigma_{xy} = \frac{e^2}{h}$ . We find the Fermi surface nesting is robust for arbitrary value of next-nearest-neighbor hopping integral. It is thus very possible that the quarter-doped graphene system will realize such an exotic ground state. We also show that the quarter-doped Hubbard model on honeycomb lattice is in exact equivalence in the weak coupling limit with the 3/4-filled Hubbard model on triangular lattice, in which similar effect is also observed.

PACS numbers: 75.10.-b, 73.43.-f, 71.27.+a

Effects of electron correlation on honeycomb lattice have attracted a lot of interest recently[1–5]. The honeycomb lattice has the smallest coordination number of 3 for a two dimensional lattice and has Dirac-type dispersion at half filling. It is a nontrivial task to understand the role of electron correlation in such a background. As an example, it is recently reported that the transition from the semimetal phase to the antiferromagnetic ordered phase in the half-filled Hubbard model on honeycomb lattice is realized in a two-step manner. An exotic spin liquid state is found in a small but finite correlation range in between the semimetal phase and the antiferromagnetic ordered phase.[1].

However, in the two dimensional graphene sheet[8, 9], which is thought to be the most natural realization of an electron system with a honeycomb lattice, the correlation effect is believed to be rather weak. Such a view is in general reasonable. However, when the Fermi energy approaches the Van Hove singularity(VHS) of the density of state, the importance of the correlation effect is much enhanced. Especially, when the system has a perfectly nested Fermi surface, an infinitesimally small interaction is enough to induce dramatic correlation effect. Recently, large electron doping on graphene system has been achieved in experiment through both chemical doping and electrolytic gating[10, 11]. It is also found by angle-resolved-photoemission measurement that the VHS is much more extended than the free electron prediction.

The density of state of the free electron on honeycomb lattice (with nearest-neighbor hopping) is shown in Fig.1. The VHS appears on both sides of the half-filled background(at 3/4 or 5/4 band filling[12]). At such special fillings, the system has a perfectly nested Fermi surface. As an example, the single particle energy on the Brillouin zone boundary is given by  $\pm t$ , where  $t$  is the hopping integral between neighboring sites. It is important to note that rather than one, there are three independent nesting vectors:  $Q_1 = \frac{1}{2}\mathbf{b}_1$ ,  $Q_2 = \frac{1}{2}\mathbf{b}_2$  and  $Q_3 = \frac{1}{2}(\mathbf{b}_1 + \mathbf{b}_2)$ ,

where  $\mathbf{b}_1$  and  $\mathbf{b}_2$  are the two elementary reciprocal vectors of the system(see Fig.1). The exact same situation also occurs on triangular lattice when the band is  $\frac{3}{4}$ -filled. In that case, an interesting magnetic insulating state with nonzero spin chirality and spontaneous quantum Hall effect is predicted[16, 17]. In this paper, we find that the exact same thing will also happen on the honeycomb lattice. In fact, we can show that both systems share the exact same low energy theory near the VHS, apart from an overall reduction of the energy scale by a factor of 2. We also find that the nesting property of the Fermi surface is robust for arbitrary value of the next-nearest-neighbor hopping integral. We thus argue that the quarter-doped graphene system has large chance to realize such an exotic spontaneous quantum Hall state.

In a magnetic ordered background with nonzero spin chirality, the motion of electron along a closed loop will experience a Berry phase(equals to the solid angle subtended by the spins along the loop), whose effect is indistinguishable from the Aharonov-Bohm phase induced by external magnetic field. Such a quantum phase is predicted to induce anomalous contribution to the Hall coefficient in systems with non-coplanar magnetic order[13–15]. In particular, when the magnetic order opens a full gap in the electron spectrum, such anomalous contribution can only take quantized values.

For the  $\frac{3}{4}$ -filled Hubbard model on triangular lattice, as the result of the Fermi surface nesting, a four-sublattice non-coplanar magnetic order is established for infinitesimally small value of electron correlation. In this state, the ordered moments in the four sublattices point along the normals of the four surfaces of a tetrahedron. The spins on each elementary triangular plaquette subtend a solid angle of  $\pi$ . In such a non-coplanar state, the electron spectrum opens a full gap and the Berry phase effect induces a quantized Hall conductance of  $\sigma_{xy} = \frac{e^2}{h}$  at zero temperature. Since the order is deduced from a weak coupling instability related to the nesting prop-

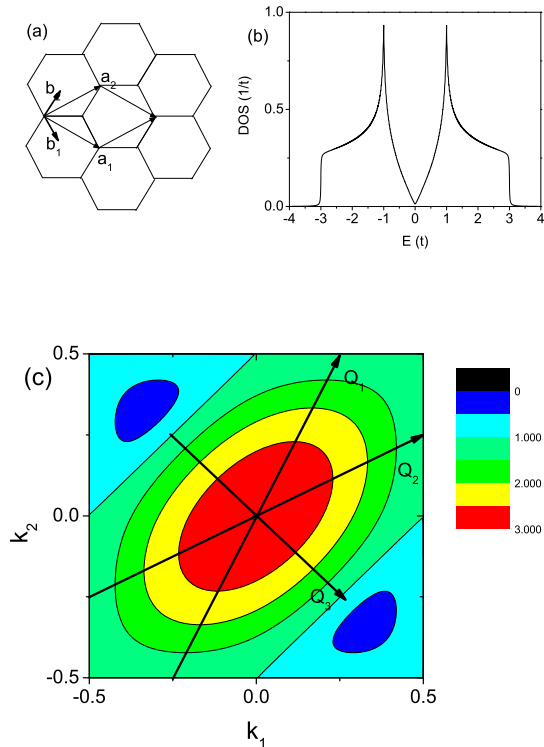


FIG. 1: The density of state and the Fermi surface of free electron on honeycomb lattice with nearest-neighbor hopping. The VHS appears at  $E = \pm t$ , which corresponds to electron filling of  $3/4$  and  $5/4$  per unit cell.

erty of the Fermi surface, it should be stable when the correlation is not too strong.

Since the system has three independent nesting vectors at the VHS, it has many different choices for developing a magnetic order. The simplest choice of Bose condensation at a single nesting vector results in a collinear magnetic state, while the non-coplanar magnetic state with the tetrahedron ordering pattern can be viewed as a state with Bose condensation on all the three nesting vectors with the same strength[16]. The tetrahedron ordering pattern can be perfectly fitted into the honeycomb lattice as shown in Fig.2. In such a state, each site is neighbored by three sites in the other three magnetic sublattices. We note that the system can also be viewed as being composed of two triangular sublattices, on each of which a tetrahedron ordering pattern is established.

To check the stability of the tetrahedron ordering pattern, we have carried out unrestricted mean field search for the quarter-doped Hubbard model on honeycomb lattice with  $12 \times 12 \times 2$  lattice sites. We have included both magnetic and charge order parameters in the optimization. On the  $12 \times 12 \times 2$  lattice, there are in total 864 variational parameters for the spin density and 288 variational parameters for the charge density to be optimized.

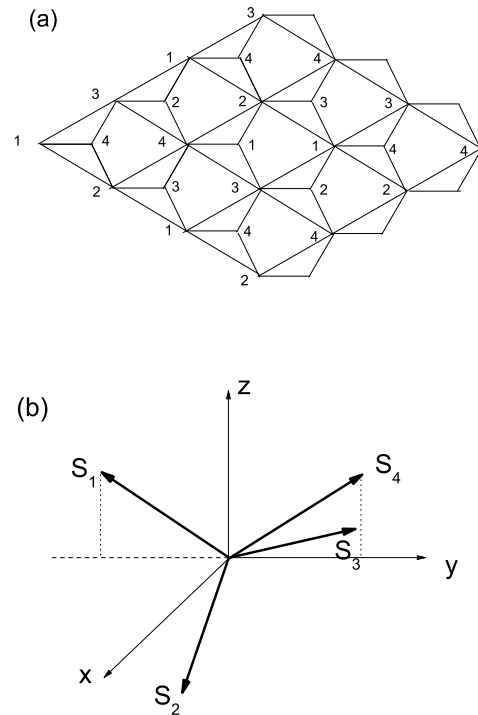


FIG. 2: Illustration of the tetrahedron magnetic ordering pattern on honeycomb lattice. The directions of the ordered moments have been chosen in such a way to make the mean field Hamiltonian as simple as possible.

We have used both the conjugate gradient method and the simulated annealing method to find the minimum of the variational energy. Both methods predict that the tetrahedron ordering pattern is the most stable one and the charge distribution is always uniform. We now present the mean field theory of this state.

In the mean field treatment, the Hubbard model on honeycomb lattice has the form,

$$H = -t \sum_{\langle i,j \rangle, \sigma} (c_{i,A,\sigma}^\dagger c_{j,B,\sigma} + h.c.) \quad (1)$$

$$- \frac{4U}{3} \sum_i \langle S_{i,A} \rangle \cdot S_{i,A} - \frac{4U}{3} \sum_j \langle S_{j,B} \rangle \cdot S_{j,B},$$

here  $S_{i,A}$  ( $S_{j,B}$ ) denotes the spin operator on site  $i$  ( $j$ ) of sublattice  $A$  ( $B$ ).

The ordered moments in the tetrahedron state can be written as

$$\langle S_{i,A} \rangle = \frac{m}{\sqrt{3}} (\vec{e}_z e^{i\mathbf{Q}_3 \cdot \mathbf{R}_i} + \vec{e}_x e^{i\mathbf{Q}_1 \cdot \mathbf{R}_i} + \vec{e}_y e^{i\mathbf{Q}_2 \cdot \mathbf{R}_i}) \quad (2)$$

$$\langle S_{j,B} \rangle = \frac{m}{\sqrt{3}} (\vec{e}_z e^{i\mathbf{Q}_3 \cdot \mathbf{R}_j} - \vec{e}_x e^{i\mathbf{Q}_1 \cdot \mathbf{R}_j} - \vec{e}_y e^{i\mathbf{Q}_2 \cdot \mathbf{R}_j}).$$

With Eq.(2), the mean field Hamiltonian in the momen-

tum space takes the form

$$H = \sum_{\mathbf{k} \in MBZ} \psi_{\text{I},\mathbf{k}}^\dagger (\Gamma_{\mathbf{k}} - \beta M) \psi_{\text{I},\mathbf{k}} + \psi_{\text{II},\mathbf{k}}^\dagger (\Gamma_{\mathbf{k}} - \beta M) \psi_{\text{II},\mathbf{k}}, \quad (3)$$

in which  $\psi_{\text{I},\mathbf{k}}^\dagger = (c_{\mathbf{k}\uparrow}^{A\dagger}, c_{\mathbf{k}\uparrow}^{B\dagger}, c_{\mathbf{k}+\mathbf{Q}_1\downarrow}^{A\dagger}, c_{\mathbf{k}+\mathbf{Q}_1\downarrow}^{B\dagger}, c_{\mathbf{k}+\mathbf{Q}_2\downarrow}^{A\dagger}, c_{\mathbf{k}+\mathbf{Q}_2\downarrow}^{B\dagger}, c_{\mathbf{k}+\mathbf{Q}_3\uparrow}^{A\dagger}, c_{\mathbf{k}+\mathbf{Q}_3\uparrow}^{B\dagger})$ ,  $\psi_{\text{II},\mathbf{k}}^\dagger = (c_{\mathbf{k}\downarrow}^{A\dagger}, c_{\mathbf{k}\downarrow}^{B\dagger}, c_{\mathbf{k}+\mathbf{Q}_1\uparrow}^{A\dagger}, c_{\mathbf{k}+\mathbf{Q}_1\uparrow}^{B\dagger}, -c_{\mathbf{k}+\mathbf{Q}_2\uparrow}^{A\dagger}, -c_{\mathbf{k}+\mathbf{Q}_2\uparrow}^{B\dagger}, -c_{\mathbf{k}+\mathbf{Q}_3\downarrow}^{A\dagger}, -c_{\mathbf{k}+\mathbf{Q}_3\downarrow}^{B\dagger})$ . The spectrum is thus explicitly two-fold degenerate.  $\Gamma_{\mathbf{k}}$  and  $M$  are  $8 \times 8$  Hermitian matrices and are given by

$$\Gamma_{\mathbf{k}} = \begin{pmatrix} \gamma_{\mathbf{k}} & 0 & 0 & 0 \\ 0 & \gamma_{\mathbf{k}+\mathbf{Q}_1} & 0 & 0 \\ 0 & 0 & \gamma_{\mathbf{k}+\mathbf{Q}_2} & 0 \\ 0 & 0 & 0 & \gamma_{\mathbf{k}+\mathbf{Q}_3} \end{pmatrix}$$

and

$$M = \begin{pmatrix} 0 & \sigma_3 & -i\sigma_3 & I \\ \sigma_3 & 0 & -I & i\sigma_3 \\ i\sigma_3 & -I & 0 & \sigma_3 \\ I & -i\sigma_3 & \sigma_3 & 0 \end{pmatrix},$$

in which  $\gamma_{\mathbf{k}} = - \begin{pmatrix} \mu & g_{\mathbf{k}} \\ g_{\mathbf{k}}^* & \mu \end{pmatrix}$ ,  $g_{\mathbf{k}} = 1 + e^{-i2\pi k_1} + e^{-i2\pi k_2}$ ,

$\sigma = \begin{pmatrix} 1 & 0 \\ 0 & -1 \end{pmatrix}$ ,  $I$  is the  $2 \times 2$  identity matrix.  $\beta = \frac{2Um}{3\sqrt{3}}$

and  $\mu$  is the chemical potential to be determined by filling concentration. In the summation, the momentum is restricted to the magnetic Brillouin zone given by  $-\frac{1}{2} \leq k_1, k_2 \leq \frac{1}{2}$  (here we have used the convention for momentum in which  $\mathbf{k} = k_1 \mathbf{b}_1 + k_2 \mathbf{b}_2$ ).

The self-consistent equation for the order parameter  $m$  is given by

$$m = \frac{1}{4\sqrt{3}N} \sum_{\mathbf{k} \in MBZ} \left[ \langle \psi_{\text{I},\mathbf{k}}^\dagger M \psi_{\text{I},\mathbf{k}} \rangle + \langle \psi_{\text{II},\mathbf{k}}^\dagger M \psi_{\text{II},\mathbf{k}} \rangle \right]. \quad (4)$$

We have solved this equation as a function of  $U/t$  at zero temperature for the quarter-doped system. The result is shown in Fig.3. The order parameter  $m$  is seen to increase with  $U/t$  from  $U/t = 0$ . This is the result of the nesting property of the Fermi surface. The tetrahedron order is thus a weak coupling instability of the system.

The tetrahedron state has a nonzero spin chirality, *i.e.*,  $\langle \mathbf{S}_i \cdot (\mathbf{S}_j \times \mathbf{S}_k) \rangle \neq 0$  for spins on neighboring sites. Electron moving on such a background will experience a nonzero Berry phase, which will induce an anomalous contribution to the Hall response of the electron system. Since the state is fully gapped, such an anomalous contribution must take quantized values of the form  $\frac{n e^2}{h}$ , where  $n$  is the total Chern-number of all the occupied bands. Now we show that  $\sigma_{xy} = \frac{e^2}{h}$  at zero temperature in this state.

The Kubo formula for the Hall conductance  $\sigma_{xy}$  is given by

$$\sigma_{xy} = \frac{e^2}{h} \frac{2\pi}{iS} \sum_{\mathbf{k}, n, m} \frac{j_{n,m}^x(\mathbf{k}) j_{m,n}^y(\mathbf{k})}{(\epsilon_n(\mathbf{k}) - \epsilon_m(\mathbf{k}))^2} (f(\epsilon_n(\mathbf{k})) - f(\epsilon_m(\mathbf{k}))), \quad (5)$$

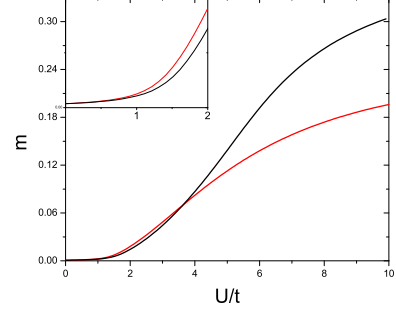


FIG. 3: The order parameter as a function of  $U/t$  at zero temperature. The black line gives the result of the quarter-filled honeycomb lattice, the red line gives the result of the 3/4-filled triangular lattice for a comparison. The inset shows the comparison in the weak coupling limit, in which the two lattices show the exact same behavior.

in which  $S$  is the area of the system.  $j_{n,m}^x(\mathbf{k})$  and  $j_{n,m}^y(\mathbf{k})$  are the matrix elements of the current operators between the  $n$ -th and the  $m$ -th eigenstate of the band Hamiltonian at momentum  $\mathbf{k}$ .  $f(\epsilon_m(\mathbf{k}))$  is the Fermi distribution function. The current operator  $j^x$  is given by

$$j^x = \sum_{\mathbf{k} \in MBZ} \psi_{\text{I},\mathbf{k}}^\dagger C_{\mathbf{k}}^x \psi_{\text{I},\mathbf{k}} + \psi_{\text{II},\mathbf{k}}^\dagger C_{\mathbf{k}}^x \psi_{\text{II},\mathbf{k}}. \quad (6)$$

$j^y$  is given by a similar expression with  $C_{\mathbf{k}}^x$  replaced by  $C_{\mathbf{k}}^y$ . Here  $C_{\mathbf{k}}^{x,y}$  are  $8 \times 8$  matrices and are given by

$$C_{\mathbf{k}}^{x,y} = \begin{pmatrix} c_{\mathbf{k}}^{x,y} & 0 & 0 & 0 \\ 0 & c_{\mathbf{k}+\mathbf{Q}_1}^{x,y} & 0 & 0 \\ 0 & 0 & c_{\mathbf{k}+\mathbf{Q}_2}^{x,y} & 0 \\ 0 & 0 & 0 & c_{\mathbf{k}+\mathbf{Q}_3}^{x,y} \end{pmatrix},$$

in which  $c_{\mathbf{k}}^{x,y} = \begin{pmatrix} 0 & v_{\mathbf{k}}^{x,y} \\ v_{\mathbf{k}}^{*x,y} & 0 \end{pmatrix}$ ,  $v_{\mathbf{k}}^x = it - \frac{it}{2}(e^{-i2\pi k_1} + e^{-i2\pi k_2})$ ,  $v_{\mathbf{k}}^y = \frac{it\sqrt{3}}{2}(e^{-i2\pi k_1} - e^{-i2\pi k_2})$ .

To calculate  $\sigma_{xy}$ , we first solve the mean field equation at finite temperature. The order parameter as a function of temperature at fixed doping and  $\frac{U}{t} = 4$  is shown in Fig.4. The mean field critical temperature is found to be  $T_c \approx 0.09t$  for this set of parameters. The Hall conductivity is also shown in Fig.4.  $\sigma_{xy}$  is found to be zero above  $T_c$  and begins to increase below  $T_c$ , following the exact same trend as the order parameter. It finally saturates to the quantized value of  $\sigma_{xy} = \frac{e^2}{h}$  at zero temperature.

The results obtained here are very similar to the results for the 3/4-filled Hubbard model on triangular lattice[16]. For example, the critical temperatures on both lattices are around  $0.09t$  for  $\frac{U}{t} = 4$ . To understand this close similarity, we note that the honeycomb lattice is actually composed of two interpenetrating triangular lattices, on each of which a tetrahedron ordering pattern is established. Actually, we can show that the quarter-doped

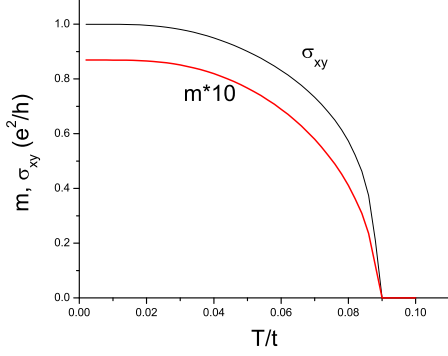


FIG. 4: The order parameter and the Hall conductance as functions of temperature at  $U/t = 4$ . Note the close similarity of these results with the results on triangular lattice[16].

Hubbard model on honeycomb lattice and 3/4-filled Hubbard model on triangular lattice are described by the same theory in the low energy limit, except for a rescaling of the overall energy scale by a factor of 2. First, we note the dispersion of the honeycomb lattice has the form

$$E_k^h = t|g(k)| = t\sqrt{3 + 2(\cos(k_1) + \cos(k_2) + \cos(k_1 - k_2))},$$

while the dispersion of the triangular lattice has the form

$$E_k^t = -2t(\cos(k_1) + \cos(k_2) + \cos(k_1 - k_2)).$$

It can then be shown that both lattices share the same dispersion relation near the VHS (where  $E_k^t = -2t$ ) apart from a factor of 2 rescaling of the energy scale. At the same time, it can be shown that the Hubbard interaction term on both lattices can be rescaled into each other in the low energy limit and the rescaling factor is also 2. In the low energy limit, the Hubbard interaction  $H_U = U \sum_i n_{i,\uparrow} n_{i,\downarrow}$  on triangular lattice is given by

$$H_U \sim U \sum_{k_i, k'_i, i} c_{k_i, \uparrow}^\dagger c_{k'_i + Q_i, \uparrow} c_{k'_i, \downarrow}^\dagger c_{k_i + Q_i, \downarrow}, \quad (7)$$

where the sum over  $i$  denotes the sum over the three patches of nested Fermi surfaces.  $k_i, k'_i$  are the momentums on the  $i$ -th patch of nested Fermi surface and  $Q_i$  denotes the nesting vector on this patch of Fermi surface. On honeycomb lattice, the Hubbard interaction takes the form of  $H_U = U \sum_i (n_{iA, \uparrow} n_{iA, \downarrow} + n_{iB, \uparrow} n_{iB, \downarrow})$ . In the low energy limit, it reduces to

$$H_U \sim U \sum_{k_i, k'_i, i} c_{A, k_i, \uparrow}^\dagger c_{A, k'_i + Q_i, \uparrow} c_{A, k'_i, \downarrow}^\dagger c_{A, k_i + Q_i, \downarrow} + U \sum_{k_i, k'_i, i} c_{B, k_i, \uparrow}^\dagger c_{B, k'_i + Q_i, \uparrow} c_{B, k'_i, \downarrow}^\dagger c_{B, k_i + Q_i, \downarrow}. \quad (8)$$

The free electron system on honeycomb lattice forms two bands with eigen-energy  $E_{\pm, k} = \pm t|g(k)|$ . If we denote the operators of the two bands as  $c_{+, k}$  and  $c_{-, k}$ , we have

$$\begin{pmatrix} c_{+, k} \\ c_{-, k} \end{pmatrix} = \frac{1}{\sqrt{2}} \begin{pmatrix} 1 & e^{i\phi_k} \\ -e^{-i\phi_k} & 1 \end{pmatrix} \begin{pmatrix} c_{A, k} \\ c_{B, k} \end{pmatrix}, \quad (9)$$

in which  $\phi_k$  is the phase of  $g(k)$ . Noting that the nested Fermi surface patches are given by  $k_1 = \frac{1}{2}$ ,  $k_2 = \frac{1}{2}$  and  $k_1 - k_2 = \frac{1}{2}$ , it is straightforward to show that  $\phi_{k_i} - \phi_{k_i + Q_i} = \pi, \pi, \text{ and } 0$  on the three patches. Thus, when the Hubbard interaction term is projected into the subspace of the  $E_+$  (or  $E_-$ ) band, the phase of its matrix element will be exact zero. Collecting all contributions, we find that in the low energy limit the Hubbard interaction takes the form

$$H_U \sim \frac{U}{2} \sum_{k_i, k'_i, i} c_{+, k_i, \uparrow}^\dagger c_{+, k'_i + Q_i, \uparrow} c_{+, k'_i, \downarrow}^\dagger c_{+, k_i + Q_i, \downarrow} + \frac{U}{2} \sum_{k_i, k'_i, i} c_{-, k_i, \uparrow}^\dagger c_{-, k'_i + Q_i, \uparrow} c_{-, k'_i, \downarrow}^\dagger c_{-, k_i + Q_i, \downarrow}. \quad (10)$$

Thus in the low energy limit, the quarter-doped Hubbard model on honeycomb lattice can be rescaled into the 3/4-filled Hubbard model on triangular lattice with a reduction of overall energy scale by a factor of 2. This explains the close similarity between the results obtained on both lattices. Note that this equivalence only holds in the weak coupling limit (see Fig.3).

Although the calculation is done at the mean field level, our conclusion that the ground state of the system is a topological insulator with a quantized Hall conductance should be robust for sufficiently small  $\frac{U}{t}$ , since the magnetic ordering is induced by the Fermi surface nesting. The situation at finite temperature is more subtle, since the Wagner-Mermin theorem prohibits spontaneous breaking of continuous symmetry at finite temperature in two dimensional systems. However, as the ordered state also breaks the discrete time reversal symmetry, possibility still exists that the spin chirality may survive even without ordered moment[18]. It is interesting to see if the spin chirality can survive at finite temperature, when the ordered moment is already washed out by thermal fluctuation.

Finally, we turn to the implications of our results on the physics of graphene. First, we note that the dispersion of the graphene system is not perfectly particle-hole symmetric. Uncertainty remains in the strength of longer rangel hopping integrals. The next-neighbor hopping integral is estimated to be in the range of  $0.02t \leq t' \leq 0.2t$ [9]. A small but finite next-next-neighbor hopping integral can also exist[19]. However, we want to emphasize that the nesting property of the quarter-doped system is robust against the introduction of next-neighbor hopping integral. The perfect nesting will only be destroyed by the next-next-neighbor hopping, which is much smaller

than the nearest and next-nearest neighboring hopping integrals. We thus believe that our result should be applicable to the graphene system.

To be more specific, we have done the mean field calculation for nonzero  $t'/t$ . The order parameter at zero temperature as a function of  $U/t$  for  $t'/t = 0.2$  and  $t'/t = -0.2$  are shown in Fig.5, in which they are compared with the result for  $t'/t = 0$ . It is seen that the tetrahedron magnetic order still develops at infinitesimally small value of interaction, no matter what is the sign of  $t'$ . The sign of  $t'$  does play a role in reducing or enhancing the magnitude of the order parameter. On the honeycomb lattice, the sign of  $t'$  will change under the particle-hole transformation. For example, electron doping in a system with positive  $t'$  is equivalent to hole doping in a system with negative  $t'$ . Thus both signs of  $t'$  are meaningful for the graphene system.

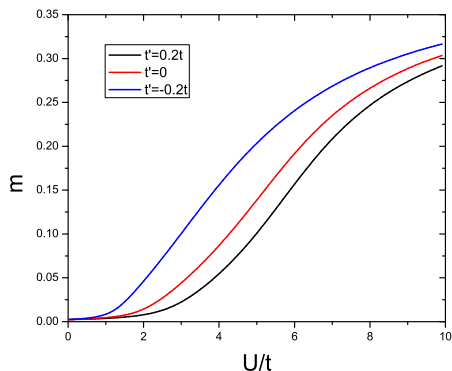


FIG. 5: The order parameter as a function of  $U/t$  for  $t'/t = 0.2, 0$ , and  $-0.2$ .

After the completion of this work[20], we noticed many related recent researches in which other ordering patterns are proposed[21–26]. Especially, a chiral d-wave superconducting order is suggested for the ground state of the quarter-doped system by RG analysis[23, 25]. However, more recent functional RG study and variational calculation show that for the quarter-doped system, the tetrahedron magnetic ordering pattern proposed in this paper enjoys a much larger condensation energy than the chiral d-wave superconducting state[26].

We conclude that the quarter-doped Hubbard model on honeycomb lattice has weak coupling instability to the formation of a magnetic insulating state with nonzero spin chirality and quantized Hall conductance as a result of the nesting property of the Fermi surface. We find the nesting property is robust against the introduction of next-nearest-neighboring hopping terms. We thus believe

that such an exotic state should be observable in quarter-doped graphene system. Such an exotic state can also act as the parent phase of even more exotic phases if we move slightly away from the VHS.

This work is supported by NSFC Grant No. 10774187 and National Basic Research Program of China No. 2007CB925001 and No. 2010CB923004.

- 
- [1] Z. Y. Meng, T. C. Lang, S. Wessel, F. F. Assaad, and A. Muramatsu, *Nature* 464, 847(2010).
  - [2] Cenke Xu and Subir Sachdev, *Phys.Rev.Lett.* 105, 057201,(2010).
  - [3] F. Wang, arXiv:1004.2693.
  - [4] Yuan-Ming Lu and Ying Ran, arXiv:1005.4229.
  - [5] Tao Li, *EPL*, 93 37007 (2011).
  - [6] G. Baskaran, *Phys. Rev. B* 65, 212505 (2002).
  - [7] A. M. Black-Schaffer and S. Doniach, *Phys. Rev. B* 75, 134512 (2007).
  - [8] K. S. Novoselov, A. K. Geim, S. V. Morozov, D. Jiang, Y. Zhang, S. V. Dubonos, I. V. Grigorieva, and A. A. Firsov, *Science* 306, 666 (2004).
  - [9] A. H. C. Neto, F. Guinea, N. M. R. Peres, K. S. Novoselov and A. K. Geim, *Rev.Mod.Phys.* 81,109(2009).
  - [10] J. L. McChesney, A. Bostwick, T. Ohta, T. Seyller, K. Horn, J. Gonzalez, and E. Rotenberg, *Phys. Rev. Lett.* 104, 136803 (2010).
  - [11] D. K. Efetov and P. Kim, *Phys. Rev. Lett.* 105, 256805 (2010).
  - [12] Here the filling fraction is defined as the number of electron per unit cell for each spin. The undoped graphene system thus has a filling fraction of 1. Note this definition is different from that used in [23], in which the undoped system has a filling fraction of 0.5.
  - [13] K. Ohgushi, S. Murakami, and N. Nagaosa, *Phys. Rev. B* 62, R6065 (2000).
  - [14] Y. Taguchi et al., *Science* 291, 2573 (2001).
  - [15] S. Raghu et al., *Phys. Rev. Lett.* 100, 156401 (2008).
  - [16] Ivar Martin and C. D. Batista, *Phys. Rev. Lett.*, *Phys. Rev. Lett.* 101, 156402 (2008).
  - [17] Yasuyuki Kato, Ivar Martin and C. D. Batista, arXiv:1009.3059.
  - [18] J. C. Domenge et al., *Phys. Rev. B* 72, 024433 (2005).
  - [19] J. González, *Phys. Rev. B* 78, 205431 (2008) .
  - [20] Tao Li, arXiv:1003.0240.
  - [21] D. Makogon, R. van Gelderen, R. Roldán and C. Morais Smith, arXiv:1104.5334.
  - [22] E. V. Castro, A. G. Grushin, B. Valenzuela, M. A. H. Vozmediano, A. Cortijo and F. D. Juan, arXiv:1105.3937.
  - [23] R. Nandkishore, L. Levitov, and A. Chubukov, arXiv:1107.1903.
  - [24] G. Murthy, E. Shimshoni, R. Shankar, and H.A. Fertig, arXiv:1108.2010.
  - [25] M. Kiesel, C. Platt, W. Hanke, D. A. Abanin, and R. Thomale, arXiv:1109.2953.
  - [26] W.S. Wang, Y.Y. Xiang, Q.H. Wang, F. Wang, F. Yang, and D.H. Lee, arXiv:1109.3884.